Chapter 8
Modelling Vegetation–Erosion Dynamics in the Mugetan Desert, Yellow River Source Zone

Yanfu Li and Zhaoyin Wang

Abstract Vegetation and aeolian sand erosion are competing and interactive factors in the management of desertification. Outcomes of these interactions affect the geomorphic tendency of desertification areas. This chapter presents a dynamic model of vegetation and aeolian sand erosion and its application in the Mugetan desertification area in the source region of Yellow River. Vegetation–erosion dynamics are assessed to develop a coupling equation of vegetation coverage and aeolian sand erosion. This model takes into account the major influence factors on the dynamics including the climate, landscape, ecological stress and human stresses. This model can be used to simulate and predict the tendencies of vegetation development and aeolian sand erosion in the research area. Results from the application of the model are used to develop the vegetation–aeolian sand erosion chart for the Mugetan desertification area. In this instance, the vegetation–aeolian sand erosion chart has a relatively large Zone C, indicating that once the vegetation coverage reaches a certain value, the capacity for self-improvement is high.

Keywords Aeolian sand erosion · Vegetation development · Ecological stresses · Vegetation–aeolian sand erosion dynamics · Modelling · Yellow River source

Y. Li
Nanjing Hydraulic Research Institute, Nanjing 210029, China
e-mail: yfli@nhri.cn

Z. Wang (✉)
State Key Laboratory of Hydroscience and Engineering,
Tsinghua University, Beijing 100084, China
e-mail: zywang@mail.tsinghua.edu.cn

8.1 Introduction

Competition between the movement of sand dunes and the establishment of vegetation is a key influence upon landscape changes in areas prone to desertification (e.g. Bendali et al. 1990; Liu et al. 2002). Mobile sand dunes damage adjacent vegetation, while vegetation cover promotes stabilization of moving sand dunes, thereby aiding the ecological restoration of desertified areas. Wind erosion, sand transport and sand accumulation influence vegetation growth and development. Wind erosion damages soil structure, reduces soil fertility and thus affects the growth of vegetation, in some instances causing plants to wither and die (Liao 1980; Jiang 1983).

Moving sand dunes are products of aeolian sand deposition. In some situations, they bury farmland and grassland, destroying adjacent vegetation. Burial beneath sand affects plant invasion, settlement, growth, distribution and seed dispersal. Aeolian sand transport may alter plant community structure, affecting processes of photosynthesis and water utilization by plants (Schenk 1999). Erosion may expose and break vegetation roots. However, vegetation can prevent or retard water and wind erosion. Primary colonizing vegetation such as moss and associated soil crusts can inhibit wind erosion. Aboveground vegetation retains soil moisture, increases surface roughness, decreases or breaks down the surface wind energy, absorbs the momentum of saltated sand particles and intercepts sand (Van de Ven et al. 1989). Underground root systems can fix the soil and improve soil structure (He and Zhao 2003; Zhang et al. 2009). This helps to stabilize or reduce rates of sand dune migration. Vegetation establishment also encourages biological life, assisting in soil development (Zhang et al. 2009).

Models that assess how vegetation cover impacts upon aeolian sand erosion can be used to assess and predict the movement of sand dunes in desertification areas, informing land management and ecological restoration programmes. Examples include the wind erosion equation (WEQ) (Woodruff and Siddoway 1965), Pasak wind erosion equations, Bocharov model, Texas erosion analysis model (TEAM) (Gregory et al. 1988), wind erosion evaluation model (WEAM), revised wind erosion equation (RWEQ) and wind erosion prediction system (WEPS) (Hagen 1991). WEQ and the Bocharov model are empirical models developed from experiments and field observations. The Texas Erosion Analysis Model (TEAM) combines theoretical model and an empirical model to form a simple process model. The WEPS system incorporates weather, crop growth, decomposition, soil, hydrology and farming subroutines, but is still under development (Yang et al. 2003; Liao et al. 2004). Simulations are commonly performed in wind tunnels to appraise the role of factors such as wind speed, air relative humidity, soil particle size, soil hardness, vegetation coverage, structural breakage of soil structure and surface slope (e.g. Dong 1998).

Some sand transport models consider the impact of vegetation coverage on wind speed and entrainment velocities for sand particle movement (Buckley 1987; Wasson and Nanninga 1986; Shi 2005; Leenders et al. 2011). Iterative coupling of

calculations of wind shear stress, sediment rate equations, conservation of mass and vegetation growth models are frequently used to simulate the formation and development processes of sand dunes under the action of vegetation (Luna et al. 2011; Durán et al. 2008).

The growth and distribution of plants are influenced by factors such as temperature, light, moisture and soil nutrients. Plants exchange material, energy and momentum with the surrounding environment. There are many plant growth models (Gates 1980; McMartrie and Wolf 1983; Zhang and Zhang 2000; Guo and Yuan 2000). These models may consider a single variable environmental factor or combinations of factors (Walker et al. 1981; Olson et al. 1985), as well as individual plants or entire vegetation communities (Sharpe et al. 1985; Li et al. 2003; Zhang and Yang 2006). Dynamic vegetation models such as the dynamic global vegetation model (DGVM) can simulate responses to environmental or climate change (Wang 2006b; Wang et al. 2009). Plant succession and ecological stresses (e.g. lethal and/or damage stresses) can also be incorporated within these models (e.g. Pedersen 1998; Wang et al. 2003a, b). Lethal stress leads to plant death and reduced vegetation coverage through factors such as forest fires, deforestation, volcanic eruptions, landslides and debris flow. Damage stress refers to reduction in vegetation vitality but not death (i.e. physiological adaptation) in response to factors such as plant diseases and insect pests, grazing, cyclones, drought and pollution (Wang et al. 2005a).

Li et al. (2009) developed a vegetation and aeolian sand coupling model that incorporated impacts of water, temperature, soil and wind. The study reported here extends this work by including qualitative estimations of ecological stresses and the impacts of human activities. Vegetation development, water erosion and the effects of soil and water conservation measures are simulated, thereby providing theoretical support for watershed management programmes (Wang et al. 2003a, 2005b, 2008; Wang 2006a). This model can be used to evaluate the ecological status and evolution tendency of desertified areas and to provide technical support for desertification control and ecological management.

8.2 Vegetation–Aeolian Sand Erosion Model

Contestations between aeolian sand erosion and vegetation development are played out at the fringes of desert areas. Moving sand dunes damage the vegetation coverage, whereas vegetation promotes stabilization of moving sand dunes and ecological restoration of desertification areas. Dynamic interactions between vegetation development and aeolian sand erosion affect the geomorphic tendency of these areas, determining whether the desert will expand or retreat. This chapter develops a coupling equation of vegetation coverage and aeolian sand erosion dynamics for desertification. In this model, vegetation coverage and the amount of aeolian sand erosion are used to represent vegetation development and aeolian sand erosion, respectively. This model can be used to simulate and predict trends

in the establishment of vegetation and aeolian sand dune movement on the fringes of desertification areas. From this, management strategies can be proposed using a vegetation–aeolian sand erosion chart.

In the fringes of desertification areas, the dynamic process between vegetation development and aeolian sand erosion is influenced by natural stresses and human activities including planting trees, felling trees and erosion reduction measures. Natural stresses and human activities play a key role in the evolution process of vegetation and aeolian sand erosion. Based on the vegetation–erosion dynamic model, assuming that the action among the stresses is independent, the coupled differential equations for the vegetation–aeolian sand erosion processes under the action of stresses are obtained as follows:

$$\begin{cases} \frac{\mathrm{d}V}{\mathrm{d}t} - aV + cE = V_R + V_\tau \\ \frac{\mathrm{d}E}{\mathrm{d}t} - bE + fV = E_\tau + E_S \end{cases} \tag{8.1}$$

in which V represents vegetation cover, E represents the rate of aeolian sand erosion (mass area^{-1} time^{-1}), V_R represents positive human stresses (e.g. reforestation; time^{-1}), V_τ represents negative human stresses (e.g. deforestation; time^{-1}), E_τ represents the reduction of aeolian sand erosion by the application of straw checkerboard barriers (mass area^{-1} time^{-2}), and E_S represents the reduction of aeolian sand erosion by the application of sand-fixation measures including sandy gravel cover and sand-protecting barriers(mass area^{-1} time^{-2}). Parameter a represents the increase of vegetation coverage under the action of vegetation (time^{-1}). As vegetation retains moisture and nutrients in soil and promotes the weathering process of fine sand, then the coverage and density of vegetation will be increased. Parameter c represents the reduction of vegetation coverage under the impact of aeolian sand erosion (length^2 mass^{-1}). Aeolian sand erosion damages soil structure and the vegetation roots. Movement of sand dunes destroys vegetation. Parameter b represents the increase of the aeolian sand erosion rate under the influence of aeolian sand erosion (time^{-1}). Aeolian sand erosion destroys the granular structure in the surface soil of a sand dune and exposes the vegetation roots. Then, the rate of aeolian sand erosion will increase. In addition, aeolian sand erosion destroys vegetation and releases the underlying fine sand, which further increases the aeolian sand erosion. Parameter f represents the decrease of the aeolian sand erosion rate under the action of vegetation (mass length^{-2} time^{-2}). Vegetation development promotes the stabilization of sand dunes and the soil-forming process. The development of surface crusts and humus layers protects the sand dunes from aeolian sand erosion.

The theoretical solution for the non-homogeneous linear ordinary differential equations is as follows:

$$V = c_1 e^{m_1 t} + c_2 e^{m_2 t}$$
$$+ e^{m_1 t} \int \left[e^{-m_1 t} e^{m_2 t} \int e^{-m_2 t} \left(\frac{\mathrm{d}(V_\tau + V_R)}{\mathrm{d}t} - b(V_\tau + V_R) - c(E_\tau + E_S) \right) \mathrm{d}t \right] \mathrm{d}t \tag{8.2}$$

$$E = c_1 \frac{a - m_1}{c} e^{m_1 t} + c_2 \frac{a - m_2}{c} e^{m_2 t}$$
$$+ e^{m_1 t} \int \left[e^{-m_1 t} e^{m_2 t} \int e^{-m_2 t} \left(\frac{\mathrm{d}(E_\tau + E_S)}{\mathrm{d}t} - a(E_\tau + E_S) - f(V_\tau + V_R) \right) \mathrm{d}t \right] \mathrm{d}t$$

(8.3)

in which c_1 and c_2 are the integral constants determined by the boundary and initial conditions, and indices of m_1 and m_2 were given as:

$$m_{1,2} = \frac{1}{2} \left[(a + b) \mp \sqrt{(a + b)^2 - 4(ab - cf)} \right]$$

(8.4)

The parameters a, c, b and f are important factors in determining the vegetation–aeolian sand erosion dynamics and the resulting vegetation–aeolian sand erosion chart. They are closely related to climate, soil characteristics and geomorphic conditions and are not related with vegetation and the erosion rate. As such, the parameters of the vegetation–aeolian sand erosion dynamic model and the vegetation–erosion chart are the same in deserts with the same climate and landform conditions. Based on the vegetation–aeolian sand erosion dynamic model, the parameters can be derived using trial-and-error methods and field gathered data. First, the vegetation coverage, V, aeolian sand erosion rate, E, vegetation ecological stress, V_τ and V_R, and reduction of aeolian sand erosion rate, E_τ and E_S, are calculated from measured and related data collected over many years. Second, the coupled differential equations of vegetation–aeolian sand erosion dynamics [Eq. (8.1)] are adapted to difference equations using a differential unit of one year. Third, the parameters a, c, b and f are derived using a trial-and-error method and measured data. Finally, the evolution of vegetation and aeolian sand erosion in the research area is applied to derive the vegetation–aeolian sand erosion chart.

8.3 Application of the Vegetation–Aeolian Sand Erosion Dynamic Model to the Mugetan Desert Area

8.3.1 The Mugetan Desert Area in the Source Area of the Yellow River

The Mugetan Desert area is located in the Gonghe Basin in the source area of the Yellow River with an area of 790 km^2 (see Fig. 8.1). Geophysical explorations indicate that the silt–sand terrane of the Gonghe Basin extends to about 1500 m thick (Xu and Xu 1983). Development of the basin reflects the collapse of the main planation surface of the plateau associated with differential uplift of the Qinghai–Tibet Plateau, with vertical deformation of up to 1700 m (Brierley et al. 2016a, Chap. 1). The Gonghe Movement caused the Yellow River to enter the Gonghe Basin around 0.11 million years ago. Since then, the Yellow River has incised into its basin via
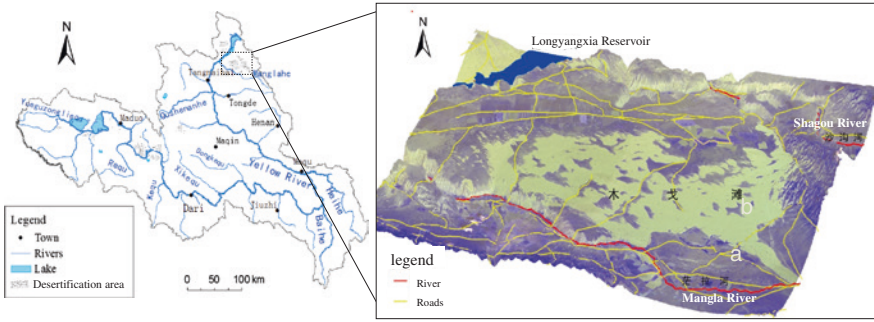
Fig. 8.1 The Mugetan Desert area in the source area of the Yellow River and surrounding streams

knickpoint retreat, at an average rate of 3.5 mm per year. At the same time, ancient alluvial fans at the edge of the basin rose at a similar rate. The resulting layered landform system extends over about 2000 m of elevation difference.

The Yellow River and its tributaries have incised the plateau for a long time, developing multistage terraces at elevations from 3000 to 2200 m asl (Brierley et al. 2016b, Chap. 3). The Mugetan Desert area is located in a high level terrace without any influence of water erosion. The area has a typical plateau continental climate (McGregor 2016 Chap. 2). The average temperature over many years was 2.4 °C, with average annual sunlight exposure of 2720 h, average rainfall of 400 mm and average annual evaporation of 1500 mm. The prevailing wind direction is south-east by south. The maximum wind speed is 14 m per year, with maximum wind speeds ≥ 7 m s^{-1} occurring on an average of 12 days per year (Guo et al. 2009, 2010).

Figure 8.2 shows the number of annual high-wind days and the maximum annual high-wind values from 1961–2009. Aeolian sandstorms are severe and have
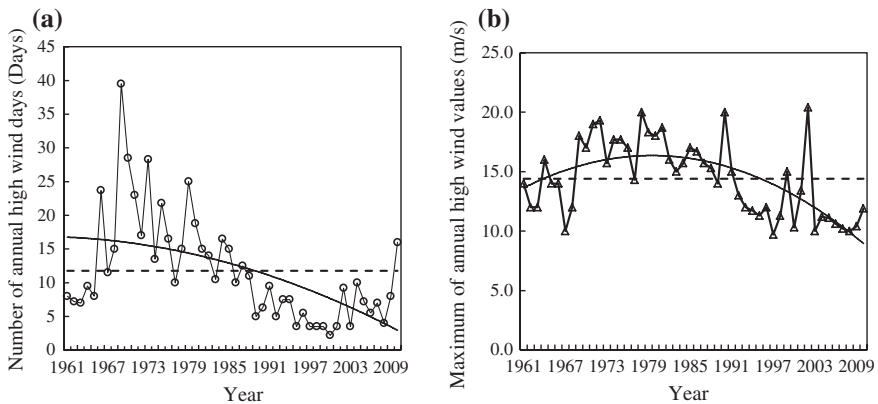

Fig. 8.2 Trend lines of the main characteristics of wind properties from 1961 to 2009. **a** Number of annual high-wind days. **b** Maximum of annual high-wind values
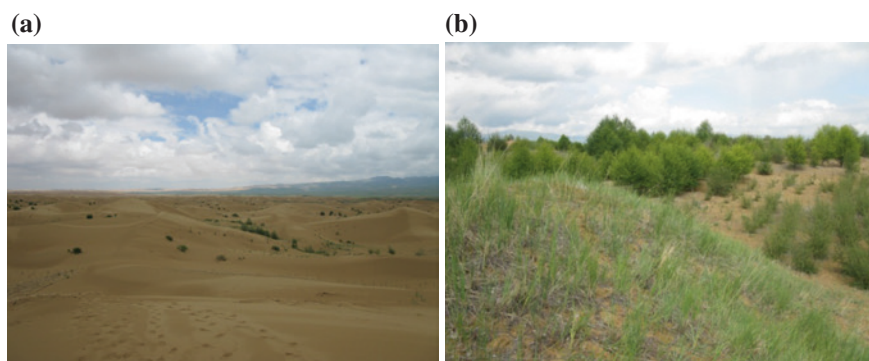
(a)   **(b)**

Fig. 8.3   The Mugetan Desert area. **a** Moving sand dunes. **b** Fixed sand deposits

become a serious threat to ecology and pasture land at the margins of the Mugetan Desert area. Vegetation restoration projects have been applied in this area since the 1970s, mainly including afforestation, laying grass squares and gravel and sand fixation. Since then, vegetation growth and aeolian sand erosion have competed with each other in the fringe area of the Mugetan Desert area. The effectiveness of these remedial effects depends on whether vegetation coverage can control wind erosion. Once the movement of sand dunes is controlled by vegetation within a certain region, the desert area will shrink, prompting recovery of the ecological environment.

Moving sand dunes, semi-fixed sand dunes and fixed sand deposits are widely distributed in the fringe area of the Mugetan Desert. The vegetation coverage of moving sand dunes is less than 5 % (Fig. 8.3a). The surface sand of a moving dune is easily moved by wind. The vegetation cover of a fixed sand deposit is over 70~80 % (Fig. 8.3b). The humus layer with a depth of 1–3 cm of a fixed sand deposit effectively retards aeolian sand erosion. The vegetation coverage of semi-fixed sand dunes is 5~60 %. Semi-fixed sand dunes with a vegetation coverage of 5~30 % are mainly covered with trees and shrubs (Fig. 8.4a). The surface sand is easily moved. Semi-fixed sand dunes with a vegetation coverage of 30~60 % are mainly covered with trees, shrubs, straw checkerboard barriers and natural restored vegetation (Fig. 8.4b).

8.3.2   Remote Sensing Analysis of Input Parameters to the Model

Based on remote sensing images, including an MSS image (1977), TM images (1988, 1996, 2003, 2005, 2007, 2008, 2009, 2010), a SPOT 2/4 image (2006) and 43 field ground-object identification spots (widely distributed around the
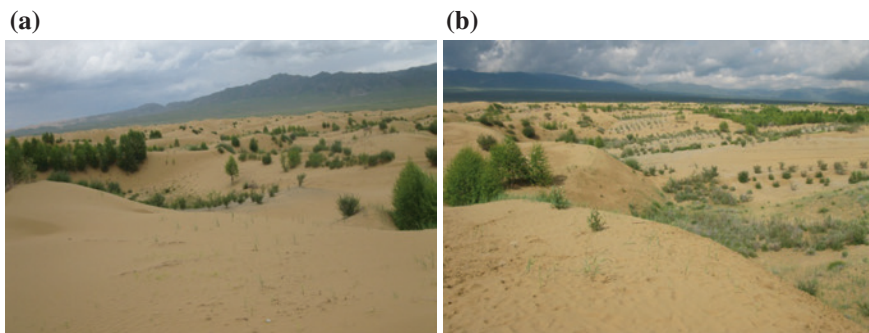
(a) (b)

Fig. 8.4 Semi-fixed sand dunes in the Mugetan Desert. **a** Vegetation coverage of 5~30 %. **b** Vegetation coverage of 30~60 %

Mugetan Desert area), the ground features were mapped over a 10-year period. The area values of every ground feature were determined using The Environment for Visualizing Images (ENVI) and an ArcGIS system (Han et al. 2009; Ma et al. 2011). Classes of ground cover were differentiated into areal assessments of moving sand dunes, semi-fixed sand dunes with a vegetation coverage of 5~30 %, semi-fixed sand dunes with a vegetation coverage of 30~60 %, fixed sand deposits with high vegetation cover, meadows, areas of bare soil and open water areas. The regions of fixed sand deposits with high vegetation coverage have a vegetation coverage of 70–80 % without any wind erosion. As the region of bare soil with developed vegetation roots has a much lower aeolian sand erosion rate than the region of aeolian sand dunes, these areas were ignored in the calculation of the aeolian sand erosion rate of the study area. The range of the fringe area of the Mugetan Desert area was identified based on the ground features measured
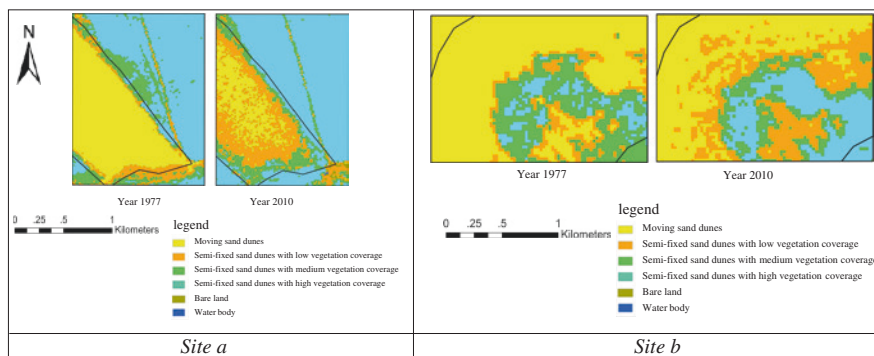

Fig. 8.5 The zoning map of the fringe area of the Mugetan Desert. Sites *a* and *b* are located in Fig. 8.1

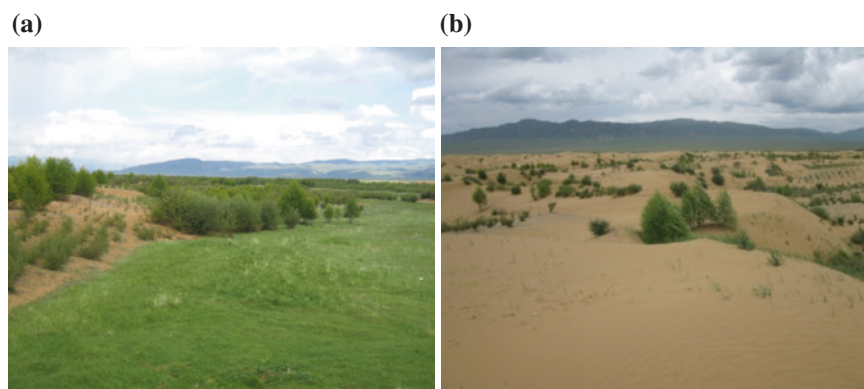**(a)**   **(b)**

Fig. 8.6   Photographs of the fringe area of the Mugetan Desert area. **a** The junction of desert and grassland. **b** The junction of the desert core area and the desert fringe area

between 1977 and 2010 within an area of 423.9 km^2. Figure 8.5a, b shows sketch maps of sites a and site b. Figure 8.6 shows feature photographs on the edges of the study area.

8.3.3 Determination of the Parameters of the Vegetation–Erosion Dynamic Model

In the model of vegetation–aeolian sand erosion dynamics (Eqs. (8.2) and (8.3)), the aeolian sand erosion rate, E, is the wind erosion sediment load on a unit area per year, regardless of the sand transport distance and accumulation process. Vegetation coverage, V, is the vegetation-covered area on a unit area and can be used to evaluate the development state of the vegetation in the study area. The records of aeolian sand erosion and vegetation in the Mugetan Desert area were rare. Vegetation coverage was estimated using remote sensing images. Aeolian sand erosion rates were approximately calculated using remote sensing images and measured aeolian sand erosion depths (from 1977 to 2010). Planting density was estimated based on engineering documents of sand-fixation projects and field investigation of afforestation areas. Engineering data and documents were used to estimate the wind erosion depth and the reduction of the aeolian sand erosion amount. Forest reservations reduced the outside impact on vegetation by building isolation areas, helping reproduction of vegetation. These vegetation processes are reflected in parameter a of the equations of the model of vegetation–aeolian sand erosion dynamics.

Based on the revised remote sensing data of many years, vegetation coverage and the area values of different locations were calculated using ArcGIS and ENVI software (Han et al. 2009; Li et al. 2009; Ma et al. 2011). Aeolian sand erosion

depths were obtained by measuring the erosion depth around the vegetation roots. In the region of moving sand dunes, aeolian sand erosion depths at four locations on the surfaces of three moving sand dunes were measured. The annual erosion rate of aeolian sand was roughly 15 cm. In the region of semi-fixed sand dunes with vegetation cover of trees and shrubs, aeolian sand erosion depths at 14 locations on the surfaces of six semi-fixed sand dunes were measured. The aeolian sand erosion depths of 5 years were obtained and used to estimate the aeolian sand erosion depths of the region of semi-fixed sand dunes with a vegetation coverage of 5~30 %. In the region of semi-fixed sand dunes with vegetation cover of trees, shrubs and straw checkerboard barriers, aeolian sand erosion depths of eleven locations on the surfaces of four semi-fixed sand dunes were measured. The aeolian sand erosion depths of 4 years were obtained and used to estimate the aeolian sand erosion depths of the region of semi-fixed sand dunes with a vegetation coverage of 30~60 %. Based on the meteorological and landform data, the annual aeolian sand erosion depths from 1977 to the present were calculated via curve fitting.

As the fringe area of the Mugetan Desert area is far away from agricultural production areas and settlements, inadvertent interference of human activities is negligible. The aeolian sand erosion depths in the fringe areas of the Mugetan desert area are approximately related to climate conditions. Wind tunnel tests and field measurements show that the greater the wind speed and number of high-wind days, the greater the wind erosion depth (Yao et al. 2001). The wind erosion amount has a quadratic relationship with wind speed, a negative quadratic power function relationship with soil particle size and an exponential function relationship with vegetation coverage. Figure 8.7 shows the fitted curves of aeolian sand erosion depth changes as a function of wind strength since 2006. The abscissa is the representative wind strength which is equal to the squared product of the annual maximum wind speed and annual number of high-wind days. Based on the meteorological data at Guinan and the fitting formula given in Fig. 8.7, wind erosion depth values since 1961 were obtained. Based on the wind erosion depth values and area values derived from different locations, the annual aeolian sand erosion rate was calculated (Table 8.1).
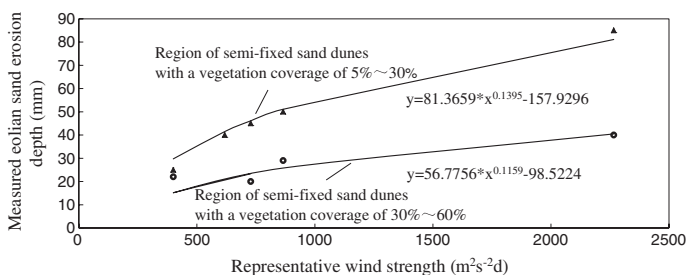

Fig. 8.7 Annual aeolian sand erosion depth changes as a function of the representative wind strength since 2006

Table 8.1 Estimated aeolian sand erosion rate and vegetation coverage in the fringe area of the Mugetan Desert area

Year	1977	1988	1996	2003	2005	2006	2007	2008	2009	2010
Aeolian sand erosion rate (E) (t km^{-2} yr^{-1})	100,876	91,513	77,562	66,874	56,037	52,747	50,814	47,975	48,201	38,214
Vegetation coverage (V) (%)	7.00	12.87	16.77	23.47	24.38	25.76	31.30	31.87	32.59	35.88

Beginning in the late 1970s, forest planting was performed through the Three-North Shelterbelt Program. Beginning in the late 1990s, many control measures were completed through several plans, including afforestation and straw checkerboard barriers (Ma 2006; Wang et al. 2000; Yang et al. 2006). From 1998 to 1999, many trees were inadvertently cut down (La 2002; La et al. 2001). In the 2000s, a series of management projects was continuously performed. Efforts to stabilize the sand dunes and restore the ecological environment included planting trees, straw checkerboard barriers, sandy gravel cover, sand-protecting barriers and forest reservation measures. The annual value of vegetation ecological stress, V_τ and V_R, and the reduction of the aeolian sand erosion rates (E_τ and E_S) were estimated based on project data, literature values and relevant measured data (see Table 8.2).

Based on the previously calculated results (including vegetation coverage, aeolian sand erosion rate, value of vegetation ecological stress and reduction of aeolian sand erosion rate), a trial-and-error method was performed many times for every adjustment of each parameter until the best-fitting value of the parameter was obtained. Derived parameters given in Eq. (8.1) for the Mugetan Desert area were determined as follows:

$$a = 0.06;\ \ c = 0.0000000987;\ \ b = 0.125;\ \ f = 16,000 \qquad (8.5)$$

A comparison of the model and measurements shows the measured and calculated processes of vegetation development and aeolian sand erosion of the Mugetan Desert area (Fig. 8.8).

Table 8.2 Annual value of vegetation ecological stress and reduction of the aeolian sand erosion rate

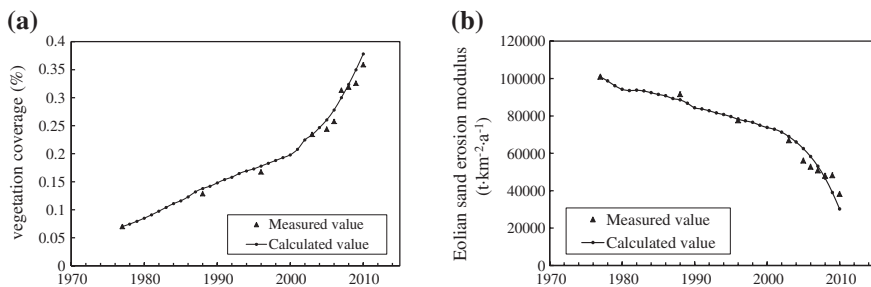| Year	Vegetation ecological stress V_τ, V_R (time^{-1})	Reduction of aeolian sand erosion rate E_τ, E_S (mass area^{-1} time^{-2})
1977~1996	$V_R = 0.2 \sim 0.5\,\%$	$E_\tau + E_S = 4000 \sim 6000\,\mathrm{t\,km^{-2}\,a^{-1}}$
1997~1999	$V_R = 0.2 \sim 0.5\,\%$; $V_\tau = 0.5 \sim 1.0\,\%$	$E_\tau + E_S = 4000 \sim 6000\,\mathrm{t\,km^{-2}\,a^{-1}}$
2000~2005	$V_R = 0.2 \sim 0.5\,\%$,	$E_\tau + E_S = 4000 \sim 7000\,\mathrm{t\,km^{-2}\,a^{-1}}$
2006~2010	$V_R = 0.5 \sim 1.0\,\%$	$E_\tau + E_S = 5000 \sim 8000\,\mathrm{t\,km^{-2}\,a^{-1}}$

(a)

(b)

Fig. 8.8 Comparison of the measured and calculated processes of (**a**) vegetation coverage and (**b**) aeolian sand erosion rate in the fringe area of the Mugetan Desert area

8.3.4 Applications of the Vegetation–Aeolian Sand Erosion Chart and Discussions

A vegetation–aeolian sand erosion chart was obtained based on the model of vegetation–aeolian sand erosion dynamics (Fig. 8.9; Wang et al. 2003b). In the case of no human-induced stresses, assuming the stress terms in Eq. (8.1) are equal to zero and $V' = \frac{dV}{dt}$, $E' = \frac{dE}{dt}$ can be rewritten as $V' = 0$, and $E' = 0$. V' and E' may be positive or negative. Therefore, the V-E plane: $V \in [0.1]$, $E \in [0, \infty)$ can be divided into 3 zones by the two lines $V' = 0$, $E' = 0$:

1. Zone A: $dV/dt < 0$, $dE/dt > 0$ (vegetation cover is decreasing and the erosion rate is increasing).
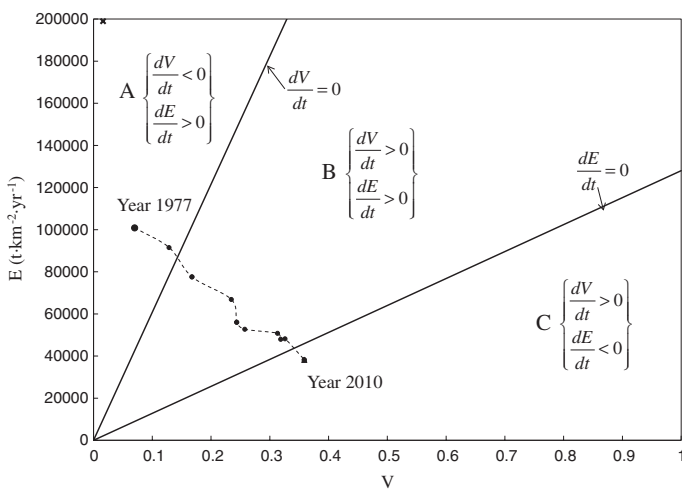

Fig. 8.9 Vegetation–aeolian sand erosion chart for the Mugetan Desert area (x—the ungoverned area of the Mugetan Desert area in 2010). E refers to erosion rate, V refers to % vegetation cover

2. Zone C: dV/dt > 0, dE/dt < 0 (vegetation cover is increasing and the erosion rate is decreasing).
3. Zone B: dV/dt > 0, dE/dt > 0 or dV/dt < 0, dE/dt < 0 (both vegetation cover and erosion rate are either increasing or decreasing).

The vegetation–erosion chart can be used to discuss the development trend of vegetation and erosion in the case of no human-induced stresses. From Eq. (8.1), two lines $V' = 0$, $E' = 0$ which divide the V-E plane: $V \in [0.1]$, $E \in [0,\infty)$ into three parts depend on the four parameters a, c, b, f:

$$E = \frac{a}{c}V; \ E = \frac{f}{b}V \qquad (8.6)$$

Evolutionary transitions from 1977–2010 show progressive reductions in sand movement over time (Fig. 8.9).

The vegetation–aeolian sand erosion chart of the source region of Yellow River has a relatively large Zone C. Figure 8.9 indicates that once the vegetation coverage reaches a certain value and the aeolian sand erosion rate decreases to a certain value, vegetation has a strong ability to self-improve, whether through natural or artificially induced vegetation succession process. As long as the vegetation does not suffer severe damage, the vegetation develops well and stabilizes the sand dunes.

In 1977, the ecological system of vegetation coverage and aeolian sand erosion in the fringe area of the Mugetan Desert area operated in Zone A is shown in Fig. 8.9. The intensity of aeolian sand erosion was far greater than the protective action of vegetation at this time. In Zone A, the vegetation cover is deteriorating and the erosion rate is increasing (i.e. desertification is getting worse). After 1977, trees were planted and straw checkerboard barriers were installed. When the vegetation cover increased to 15 % and the aeolian sand erosion rate reduced to less than 85,000 t km^2 y^{-1}, vegetation is able to control the moving sand dunes. In Zone B, the vegetation cover is in an unstable state. Both vegetation cover and erosion are increasing. If erosion increases faster or human stresses cause deforestation and erosion continues to increase, the ecological system may enter Zone A. If vegetation increases faster or human controls are applied to erosion, such as reforestation, the ecological system may enter Zone C.

Since the 1980s, the vegetation projects became effective in the fringe area of the Mugetan Desert. The vegetation coverage increased year by year, gradually reducing aeolian sand movement. When the vegetation cover increased to 35 % and the aeolian sand erosion rate reduced to less than 40,000 t km^2 yr^{-1}, the ecological system entered Zone C. In Zone C, the ecological system moves towards complete vegetation cover with an aeolian sand erosion rate of zero.

Figure 8.9 shows the ecological system now lies on the edge of Zone C (assuming no change in status since 2010). Sand dunes are controlled by vegetation, but are not stable. Vegetation management should continue to be intensively performed until the vegetation develops to rapidly stabilize the aeolian sand dunes. Then, under the action of developed vegetation, the sand dunes in the fringe area

of the Mugetan Desert will gradually be stabilized and desert expansion will be stopped.

Point "**x**" on the top left-hand side of Fig. 8.9 is the typical position for most parts of the Mugetan Desert area. As this is far removed from area C, afforestation is unlikely to stabilize sand dunes in its own right. At present, it is necessary to control aeolian sand erosion and push point "**x**" to the right by many measures. When the aeolian sand erosion rate is reduced to less than 85,000–100,000 t $km^2\, y^{-1}$, vegetation management could then make the ecological systems of most of the Mugetan Desert area enter Zone C. When the aeolian sand erosion rate is reduced to less than 40,000 t $km^2\, y^{-1}$, vegetation becomes the main control on erosion. The vegetation–aeolian sand erosion chart also shows that desert management could start from the edges of the desert and gradually advance towards the centre of the desert. First, the ecological system of the fringe area of desert must enter area C. Management strategies can then progressively advance towards the desert core. The approach outlined here could provide a valuable starting point to appraise the effectiveness of vegetation management strategies to arrest desertification processes elsewhere in the Upper Yellow River Basin.

References

Bendali, F., Floret, C., Le Floch, E., et al. (1990). The dynamics of vegetation and sand mobility in arid regions. *Journal of Arid Environments, 18*, 21–32.

Brierley, G. J., Li, X., Cullum, C., et al. (2016a). Introduction: Landscape and ecosystem diversity in the Yellow River Source Zone. In G. J. Brierley, X. Li, C. Cullum, et al. (Eds.), *Landscape and ecosystem diversity, dynamics and management in the Yellow River Source Zone*. (pp. 1–34). Berlin: Springer.

Brierley, G. J., Yu, G. A., & Li, Z. W. (2016b). Geomorphic diversity of rivers in the Upper Yellow River Basin. In G. J. Brierley, X. Li, C. Cullum, et al. (Eds.), *Landscape and ecosystem diversity, dynamics and management in the Yellow River Source Zone*. (pp. 59–78). Berlin: Springer.

Buckley, R. (1987). The effect of sparse vegetation on the transport of dune sand by wind. *Nature, 325*, 426–428.

Dong, Z. B. (1998). Establishing statistic model of wind erosion on small watershed basis. *Bulletin of Soil and Water Conservation, 18*, 55–62 (in Chinese).

Durán, O., Silva, M. V. N., Bezerra, L. J. C., et al. (2008). Measurements and numerical simulations of the degree of activity and vegetation cover on parabolic dunes in north-eastern Brazil. *Geomorphology, 102*, 460–471.

Gates, D. J. (1980). Competition between two types of plants located at random on a lattice. *Mathematical Biosciences, 48*, 157–194.

Gregory, J. M., Borrelli, J., & Fedler, C. B. (1988). Team: Texas erosion analysis model. In *Proceedings, 1988 Wind Erosion Conference* (pp. 88–103). Lubbock: Texas Tech University.

Guo, S. S., He, L. B., & Xu, Z. F. (2010). Variety trend analysis of sunshine hours in Guinan County in recent 50 Years. *Journal of Anhui Agricultural Sciences, 38*, 8530–8532. 8538 (in Chinese).

Guo, R. H., & Yuan, X. F. (2000). Hopf bifurcation for a ecological mathematical model on microbe populations. *Applied Mathematics and Mechanics, 21*, 693–700 (in Chinese).

Guo, L. Y., Zhong, C., Ding, S. X., et al. (2009). Local climate changes and their impacts on grassland degradation in Gonghe basin of Guinan county of Qinghai province in past half-century. *Chinese Journal of Agrometeorology, 230*, 147–152 (in Chinese).

Hagen, L. J. (1991). A wind erosion prediction system to meet the users need. *Journal of Soil and Water Conservation, 46*, 107–111.

Han, H. H., Yang, T. B., & Wang, Y. (2009). Dynamic analysis of land use and landscape pattern changes in Guinan county, Qinghai, in the past 30 years. *Process in Geography, 28*, 207–215.

He, Z. B., & Zhao, W. Z. (2003). Characteristics of soil moisture of different vegetation types in initial stage of fixed sand dune of semi-arid region. *Journal of Soil and Water Conservation, 17*, 164–167 (in Chinese).

Jiang, J. (1983). Research on biology and physiology characteristics of main sand-fixation plant in Shapotou. *Forest Science, 19*, 113–120 (in Chinese).

La, Y. L. (2002). The current situation of grassland ecological environment and its control strategies. *Pratacultural Science, 19*, 1–4 (in Chinese).

La, Y. L., Liang, Z. Y., & Banma, D. J. (2001). Alpine grassland desertification and control method and countermeasure of Guinan County. *Qinghai Prataculture, 11*, 41–45 (in Chinese).

Leenders, J. K., Sterk, G., & Van Boxel, J. H. (2011). Modelling wind-blown sediment transport around single vegetation elements. *Earth Surface Processes and Landforms, 36*, 1218–1229.

Li, Z. S., Wang, Y., & He, L. (2009). Vegetation-erosion process in semiarid region: Dynamical models. *Journal of Desert Research, 29*, 23–30 (in Chinese).

Li, Z. Z., Wang, W. X., & Xu, C. L. (2003). The dynamic model of crop growth system and numerical simulation of crop growth process under the multi-environment external force action. *Applied Mathematics and Mechanics, 24*, 644–652 (in Chinese).

Liao, C. Y. (1980). *Research on the choice machine characteristics of several sand-fixation plants. Quicksand quality research* (pp. 60–120). Ningxia: Ningxia People's Publishing House (in Chinese).

Liao, C. Y., Li, J., & Zheng, F. L. (2004). Research history and trend of wind erosion prediction abroad. *Research of Soil and Water Conservation, 11*, 50–53 (in Chinese).

Liu, Z. M., Zhao, X. Y., & Liu, X. M. (2002). The relation between interference and vegetation. *Acta Prataculturae Sinica, 11*, 1–9 (in Chinese).

Luna, M. C. D. M., Parteli, E. J. R., Durán, O., et al. (2011). Model for the genesis of coastal dune fields with vegetation. *Geomorphology, 129*, 215–224.

Ma, J. H. (2006). *An ecological oasis with an area of 18 million mu was completed in Guinan*. Qinghai news network, http://news.sina.com.cn/c/2006-07-06/08449385326s.shtml (in Chinese).

Ma, Y. F., Yan, P., & Zhang, D. S. (2011). Pattern of aeolian-fluvial interaction in Gonghe basin, Qinghai Province based on GIS. *Journal of Arid Land Resources and Environment, 25*, 151–156 (in Chinese).

McGregor, G. R. (2016). Climate variability and change in the Sanjiangyuan region. In G. J. Brierley, X. Li, C. Cullum, et al. (Eds.), *Landscape and ecosystem diversity, dynamics and management in the Yellow River Source Zone*. (pp. 35–58). Berlin: Springer.

McMartrie, R., & Wolf, L. (1983). A model of competition between trees and grass for radiation, water and nutrients. *Annals of Botany, 52*, 449–458.

Olson, R. L. J., Sharpe, P. J. H., & Wu, H. (1985). Whole-plant modelling: A continuous-time Markov (CTM) approach. *Ecological Modelling, 29*, 171–187.

Pedersen, B. S. (1998). Modeling tree mortality in response to short- and long-term environmental stresses. *Ecological Modelling, 105*, 347–351.

Schenk, H. J. (1999). Clonal splitting in desert shrubs. *Plant Ecology, 141*, 41–52.

Sharpe, P. J. H., Walker, J., Penridge, L. K., et al. (1985). A physiologically based continuous-time Markov approach to plant growth modelling in semi-arid woodlands. *Ecological Modelling, 29*, 189–213.

Shi, X. F. (2005). *Relation between vegetation conditions and eolian sand activities in north semiarid regions. Master Dissertation*. Beijing: Life and Environmental Science College of Central University for Nationalities (in Chinese).

Van de Ven, T. A. M., Fryrear, D. W., & Spaan, W. P. (1989). Vegetation characteristics and soil loss by wind. *Journal of Soil and Water Conservation, 44*, 347–349.

Walker, B. H., Ludwig, D., Holling, C. S., et al. (1981). Stability of semi-arid savanna grazing systems. *Journal of Ecology, 69*, 473–498.

Wang, F. X. (2006a). Research on the vegetation-erosion dynamics and its application to typical erosion areas of China. Doctoral Dissertation, Tsinghua University, China.

Wang, X. M. (2006b). The international development trend of dynamic vegetation model. *Science Journalism, 5*, 18–20 (in Chinese).

Wang, Z. Y., Guo, Y. B., Li, C. Z., et al. (2005a). Vegetation-erosion chart and its application in typical watershed in China. *Advances in Earth Science, 20*, 149–157 (in Chinese).

Wang, X. F., Ma, M. G., & Yao, H. (2009). The research progress of dynamic global vegetation model. *Journal of Remote Sensing Technology and Application, 24*, 246–251 (in Chinese).

Wang, Z. Y., Wang, G. Q., & Gao, J. (2003a). An ecological dynamics model of vegetation evolution in erosion area. *Acta Ecologica Sinica, 23*, 98–105 (in Chinese).

Wang, Z. Y., Wang, G. Q., & Huang, G. H. (2008). Modeling of state of vegetation and soil erosion over large areas. *International Journal of Sediment Research, 23*, 181–196 (in Chinese).

Wang, Z. Y., Wang, G. Q., Li, C. Z., et al. (2003b). Preliminary exploration and application of the vegetation and erosion dynamics. *Science in China (Series D), 33*, 1013–1023 (in Chinese).

Wang, Z. Y., Wang, G. Q., Li, C. Z., et al. (2005b). A preliminary study on vegetation-erosion dynamics and its applications. *Science in China (Series D Earth Sciences), 48*, 689–700 (in Chinese).

Wang, Z. T., Zhu, C. Y., Yang, Z. W., et al. (2000). A comprehensive summary of control techniques and experience of moving sand dunes in Huangshatou in Guinan. *Science and Technology of Qinghai Agriculture and Forestry, 3*, 45–47 (in Chinese).

Wasson, R. J., & Nanninga, P. M. (1986). Estimating wind transport sand on vegetated surface. *Earth Surface Processes and Landforms, 11*, 505–514.

Woodruff, N. P., & Siddoway, F. H. (1965). A wind erosion equation. *Soil Science Society of America Proceedings, 29*, 602–608.

Xu, S. Y., & Xu, D. (1983). Eolian sand accumulation in east bank of Qinghai Lake. *Journal of Desert Research, 3*, 11–17 (in Chinese).

Yang, H. X., Lu, Q., Wu, B., et al. (2006). Ecological restoration in alpine sandy lands of Gonghe basin, Qinghai Province. *Science of Soil and Water Conservation, 4*, 7–12 (in Chinese).

Yang, X. C., Yan, P., & Liu, L. Y. (2003). Advances and commentaries on wind erosion of soil. *Agricultural Research in the Arid Areas, 21*, 147–153 (in Chinese).

Yao, H. L., Yan, D., Hu, X. L., et al. (2001). Research on the law of wind erosion and deposition of sediment in moving sand dunes in Maowusu sandy land. *Mongolia Forestry Science and Technology, 1*, 3–9 (in Chinese).

Zhang, H. J., Liu, Z. G., & Gong, H. P. (2009). Spatiotemporal change of soil water in fixed sand dune. *Journal of Inner Mongolia Forestry Science and Technology, 35*, 23–26 (in Chinese).

Zhang, C. Q., & Yang, C. (2006). Simulation of plant growth and mathematical modeling study. *Acta Scientiarum Naturalium Universities Neimongol, 37*, 435–440.

Zhang, Y. P., & Zhang, J. T. (2000). The permanence of nonperiodic predator-prey system of three species Lotka-Volterra. *Applied Mathematics and Mechanics, 21*, 792–797 (in Chinese).